Report

Current Biology

Early Pheromone Experience Modifies a Synaptic Activity to Influence Adult Pheromone Responses of *C. elegans*

Highlights

- Early pheromone exposure modulates behavioral responses to the pheromone as adults
- Pheromone experience is imprinted as increased synaptic activity
- The *odr-2* GPI-linked signaling protein mediates pheromone imprinting

Authors

Myeongjin Hong, Leesun Ryu, Maria C. Ow, ..., Piali Sengupta, Sarah E. Hall, Kyuhyung Kim

Correspondence

khkim@dgist.ac.kr

In Brief

Hong et al. show that early pheromone experience in *C. elegans* hermaphrodites is imprinted via alteration of activity of a single synaptic connection and, in turn, modulates behavioral responses to the pheromone as adults.

Hong et al., 2017, Current Biology *27*, 3168–3177
October 23, 2017
http://dx.doi.org/10.1016/j.cub.2017.08.068

CellPress

CellPress

Current Biology
Report

Early Pheromone Experience Modifies a Synaptic Activity to Influence Adult Pheromone Responses of *C. elegans*

Myeongjin Hong,[1,8] Leesun Ryu,[1,8] Maria C. Ow,[2] Jinmahn Kim,[1] A Reum Je,[3] Satya Chinta,[4] Yang Hoon Huh,[3] Kea Joo Lee,[5] Rebecca A. Butcher,[4] Hongsoo Choi,[6] Piali Sengupta,[7] Sarah E. Hall,[2] and Kyuhyung Kim[1,9,*]

[1]Department of Brain and Cognitive Sciences, DGIST, Daegu 42988, Republic of Korea
[2]Department of Biology, Syracuse University, Syracuse, NY 13244, USA
[3]Center for Electron Microscopy Research, Korea Basic Science Institute, Cheongju-si, Chungcheongbuk-do 28119, Republic of Korea
[4]Department of Chemistry, University of Florida, Gainesville, FL 32611, USA
[5]Korea Brain Research Institute, Daegu 41068, Republic of Korea
[6]Robotics Engineering Department, DGIST, Daegu 42988, Republic of Korea
[7]Department of Biology and National Center for Behavioral Genomics, Brandeis University, Waltham, MA 02454, USA
[8]These authors contributed equally
[9]Lead Contact
*Correspondence: khkim@dgist.ac.kr
http://dx.doi.org/10.1016/j.cub.2017.08.068

SUMMARY

Experiences during early development can influence neuronal functions and modulate adult behaviors [1, 2]. However, the molecular mechanisms underlying the long-term behavioral effects of these early experiences are not fully understood. The *C. elegans* ascr#3 (asc-ΔC9; C9) pheromone triggers avoidance behavior in adult hermaphrodites [3–7]. Here, we show that hermaphrodites that are briefly exposed to ascr#3 immediately after birth exhibit increased ascr#3-specific avoidance as adults, indicating that ascr#3-experienced animals form a long-lasting memory or imprint of this early ascr#3 exposure [8]. ascr#3 imprinting is mediated by increased synaptic activity between the ascr#3-sensing ADL neurons and their post-synaptic SMB motor neuron partners via increased expression of the *odr-2* glycosylated phosphatidylinositol (GPI)-linked signaling gene in the SMB neurons. Our study suggests that the memory for early ascr#3 experience is imprinted via alteration of activity of a single synaptic connection, which in turn shapes experience-dependent plasticity in adult ascr#3 responses.

RESULTS

Adult *C. elegans* Transiently Exposed to ascr#3 during Larval Stages Exhibits Increased acsr#3 Pheromone Avoidance

To assess whether early experience of pheromones affects ascr#3 avoidance behavior in adult worms, we transiently exposed first larval stage (L1) wild-type worms to ascr#3 and examined their responses to ascr#3 as adults (Figure 1A; see STAR Methods). To test avoidance, a pheromone diluted in buffer was applied to a freely moving animal, and the fraction of animals that reverse was calculated (drop test assay; see STAR Methods) [9]. Pre-exposure to 600 nM ascr#3 during the L1 stage significantly improved adult avoidance of ascr#3 at concentrations that elicit only weak avoidance by adults that were not similarly pre-exposed but did not further increase avoidance at higher ascr#3 concentrations (Figure 1B). Increased ascr#3 avoidance appeared to be mediated by increased long reversals and omega turns, but not short reversals in pre-exposed animals (Figure S1A). Henceforth, we calculate increased avoidance as a learning index (LI; pre-exposed reversing rate minus naive reversing rate/100) (Figure 1C).

We next defined the optimal ascr#3 concentration that elicits the pre-exposure effect. Animals exhibited maximal adult ascr#3 avoidance when they were pre-exposed to ascr#3 concentrations higher than 600 nM (Figure 1D) [4]. Although exposure of L1 larvae to ascr#3 pheromone also promotes entry into the alternate dauer developmental stage, we note that the conditions used for imprinting are distinct from those used for dauer induction and few if any ascr#3-imprinted animals enter into the dauer stage. These results indicate that early experience of ascr#3 pheromone appears to be translated into behavioral changes in the adult stage of hermaphrodites, suggesting that ascr#3-experienced animals form a long-lasting memory or imprint for ascr#3. Wild-type *C. elegans* males exhibit neutral responses to 100 nM ascr#3 [7, 10]. We found that ascr#3-experienced adult males continue to exhibit neutral responses to 100 nM ascr#3 (Figure S1B), indicating that early ascr#3 experience appears to increase ascr#3 avoidance only by adult hermaphrodites, but not by adult males.

The Memory for ascr#3 Is Acquired during the L1 Larval Stage

To determine whether the long-lasting memory for ascr#3 is formed during a specific developmental time window, worms were pre-exposed to ascr#3 at multiple developmental stages, and their ascr#3 responses were assessed as adults. All assays were conducted by pre-exposing animals to 600 nM pheromone

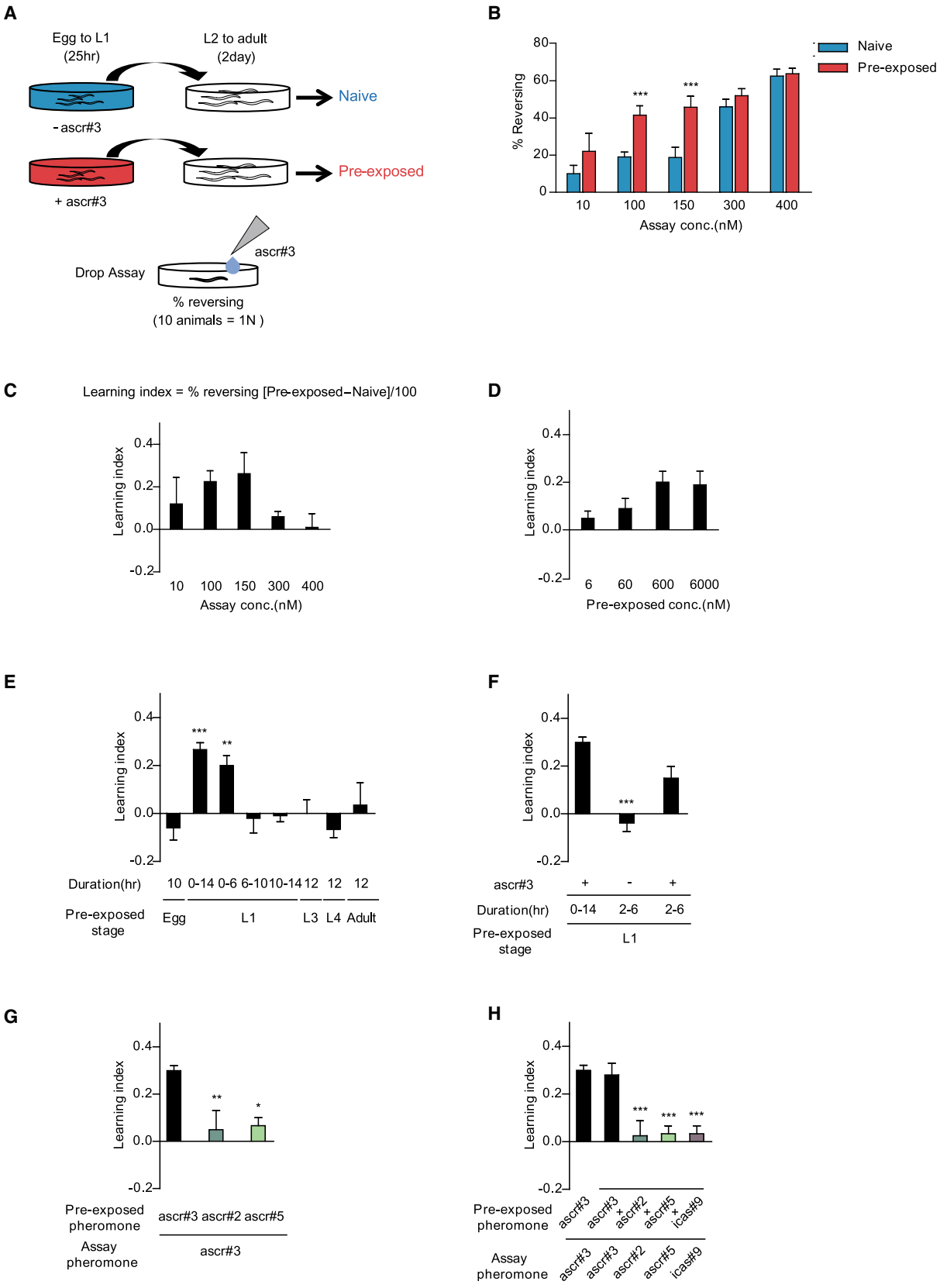

(legend on next page)

and assessing responses to 100 nM pheromone, unless noted otherwise.

Compared to the L1 stage, ascr#3 pre-exposure at the L3, L4, or adult stages did not enhance ascr#3 avoidance in adults (Figure 1E), suggesting that the L1 stage is critical for acquiring the ascr#3 memory. We could not test the L2 stage because of complexity with dauer formation [11]. We further defined the time window within the L1 stage necessary for this behavior and found that pre-exposure in a defined time period during the early L1 stage (up to 6 hr following hatching at 20°C) appears to represent the critical period for formation of the ascr#3 memory (Figure 1E). More specifically, exposure of ascr#3 to worms at 2–6 hr after birth appears to be necessary and sufficient for the increased ascr#3 avoidance (Figure 1F).

C. elegans secretes additional pheromones, including ascr#2, ascr#5, and icas#9. Similar to ascr#3, these pheromones are also potent inducers of entry into the alternate dauer developmental stage under limiting food conditions [4]. Pre-exposure to 600 nM ascr#2 or ascr#5 alone did not affect ascr#3 avoidance by adults, suggesting that pheromone imprinting does not reflect a memory of general unfavorable dauer-inducing conditions but specifically encodes experience of the ascr#3 pheromone (Figure 1G). Pre-exposure to mixtures of ascr#2, ascr#5, and icas#9 with ascr#3 also did not affect ascr#3 imprinting, further supporting that imprinting is specific to ascr#3 (Figure 1H). Moreover, pre-exposure to ascr#2 did not result in altered adult avoidance of ascr#2 (Figure S1C), further confirming specificity of this process to ascr#3. In addition, pre-exposure to ascr#3 did not affect high-osmolality glycerol avoidance (Figure S1D), suggesting that early ascr#3 experience does not affect broad avoidance behaviors to other repulsive chemicals by adults. However, we are unable to exclude the possibility that imprinting by other ascarosides may occur at developmental stages other than the L1 stage.

Because the memory for a specific pheromone component is acquired only at the critical developmental period, we further define this altered ascr#3 avoidance as sensory imprinting [8]. Interestingly, when animals recovered from the developmentally arrested dauer stage that was induced by limited food supply in the presence of pheromones, including ascr#3, at the L1 and L2 stages, their ascr#3 avoidance was comparable to or even weaker than that of naive animals (Figure S1E) [11]. These data indicate that the ascr#3 imprint appears to be removed following dauer experience and/or ascr#3 imprinting requires non-dauer-inducing conditions at the L1 stage. Moreover, it is likely that passage through the dauer stage results in genome-wide changes in gene expression patterns [12, 13], which may mask or erase ascr#3-imprinting phenotypes.

We next investigated perdurance of the ascr#3 memory. We found that pre-exposed 3- or 6-day-old adults still exhibited increased ascr#3 avoidance (Figure S1F). We also asked whether memories are transmitted to the next generation but found that progeny from imprinted mothers did not exhibit improved ascr#3 avoidance (Figure S1G). These results indicate that the ascr#3 imprint lasts with aging but is not inherited under these assay conditions.

odr-2 Acts in the SMB Neurons to Increase ascr#3 Avoidance in ascr#3-Imprinted Animals

We next performed a candidate gene search to identify genes and molecules required for ascr#3 imprinting. We first tested genes that have been shown to be required for distinct forms of learning and memory in *C. elegans*. These include the *egl-4* (cyclic guanosine monophosphate [GMP]-dependent protein kinase) gene implicated in sensory adaptation, the *casy-1* (calsyntenin) gene involved in associative learning, and the *sra-11* (7-TM G-protein-coupled receptor), *ttx-3* (LIM homeodomain protein), or *tdc-1* (tyrosine decarboxylase) genes involved in olfactory imprinting [14–17]. However, loss of function of these genes did not affect ascr#3 imprinting (Figure S2A).

In the course of analyzing mutants defective in odorant responses, we found that *odr-2* (*n2145*) [18, 19] mutants exhibited defects in ascr#3 imprinting, although the ability of these mutants to avoid ascr#3 was unaffected (Figures 2A and 2B). The ascr#3 imprinting defects in *odr-2* mutants were fully rescued upon expression of wild-type *odr-2* cDNA driven under its upstream regulatory sequences (Figure 2C). The *odr-2* gene encodes a membrane-associated protein related to the Ly-6 (leukocyte antigen-6) superfamily of GPI (glycosylated phosphatidylinositol)-linked proteins, and *odr-2* mutants have previously been shown to exhibit decreased chemotaxis toward a set of volatile attractive chemicals [19]. *odr-2* is expressed in a set of head neurons, including RIG, RME, and SMB [19, 20]. To determine where ODR-2 acts to regulate ascr#3 imprinting, we tested transgenic animals expressing *odr-2* wild-type sequences for

Figure 1. Transient Exposure to the ascr#3 Pheromone after Birth Specifically Enhances ascr#3-Avoidance Behavior of Adults

(A) Experimental scheme of pheromone imprinting assay. The animals are exposed to dH2O (naive: shown in blue) and ascr#3 diluted with dH2O (pre-exposed: shown in red) from egg to the L1 stage. The percentage of reversal is calculated by measuring avoidance frequencies to ascr#3 exposure at the adult stage.

(B and C) Percentage of reversal (B) and learning index (C) of naive and pre-exposed adult animals to 10 nM, 100 nM, 150 nM, 300 nM, and 400 nM ascr#3. Learning index is calculated by the percentage of the reversal rate of pre-exposed minus the reversal rate of naive divided by 100. *** indicates different ascr#3 avoidance from naive at $p < 0.001$ by one-way ANOVA with Bonferroni's post hoc test. n = 50–200 each.

(D) Learning index of adult animals pre-exposed to 6 nM, 60 nM, 600 nM, and 6,000 nM ascr#3 at L1. n = 80–200 each.

(E) Learning index of adult animals pre-exposed to 600 nM ascr#3 at different developmental stages. Exposure times during the specific developmental stage are indicated as egg (10 hr), L3 (12 hr), L4 (12 hr), and adult (12 hr). For the L1 stage, exposure times are indicated as between starting and ending time of pheromone exposure. ** and *** indicate different from egg (10 hr) at $p < 0.01$ and $p < 0.001$ by one-way ANOVA with Dunnett's post hoc test, respectively. n = 30–190 each.

(F) Learning index of adult animals exposed to ascr#3 for 4 hr in the L1 stage. Pre-exposure for 2∼6 hr in the L1 stage is sufficient for ascr#3 imprinting. *** indicates different from ascr#3 pre-exposure for 14 hr at $p < 0.001$ by one-way ANOVA with Dunnett's post hoc test. n = 80–120 each.

(G and H) Learning index of adult animals pre-exposed and/or assayed with other pheromone components. Animals are pre-exposed to either 600 nM ascr#3, ascr#2, or ascr#5 and assayed with 100 nM ascr#3 (G) and pre-exposed to pheromone mixture containing 600 nM ascr#3, ascr#2, ascr#5, and icas#9 and assayed with 100 nM ascr#3, ascr#2, ascr#5, or icas#9 (H). *, **, and *** indicate different from the control (ascr#3 pre-exposed and ascr#3 assayed) at $p < 0.05$, $p < 0.01$, and $p < 0.001$, respectively, by one-way ANOVA with Dunnett's post hoc test. (G) n = 30–100 each. (H) n = 30–50 each.

In (B)–(H), error bars represent SEM. See also Figure S1.

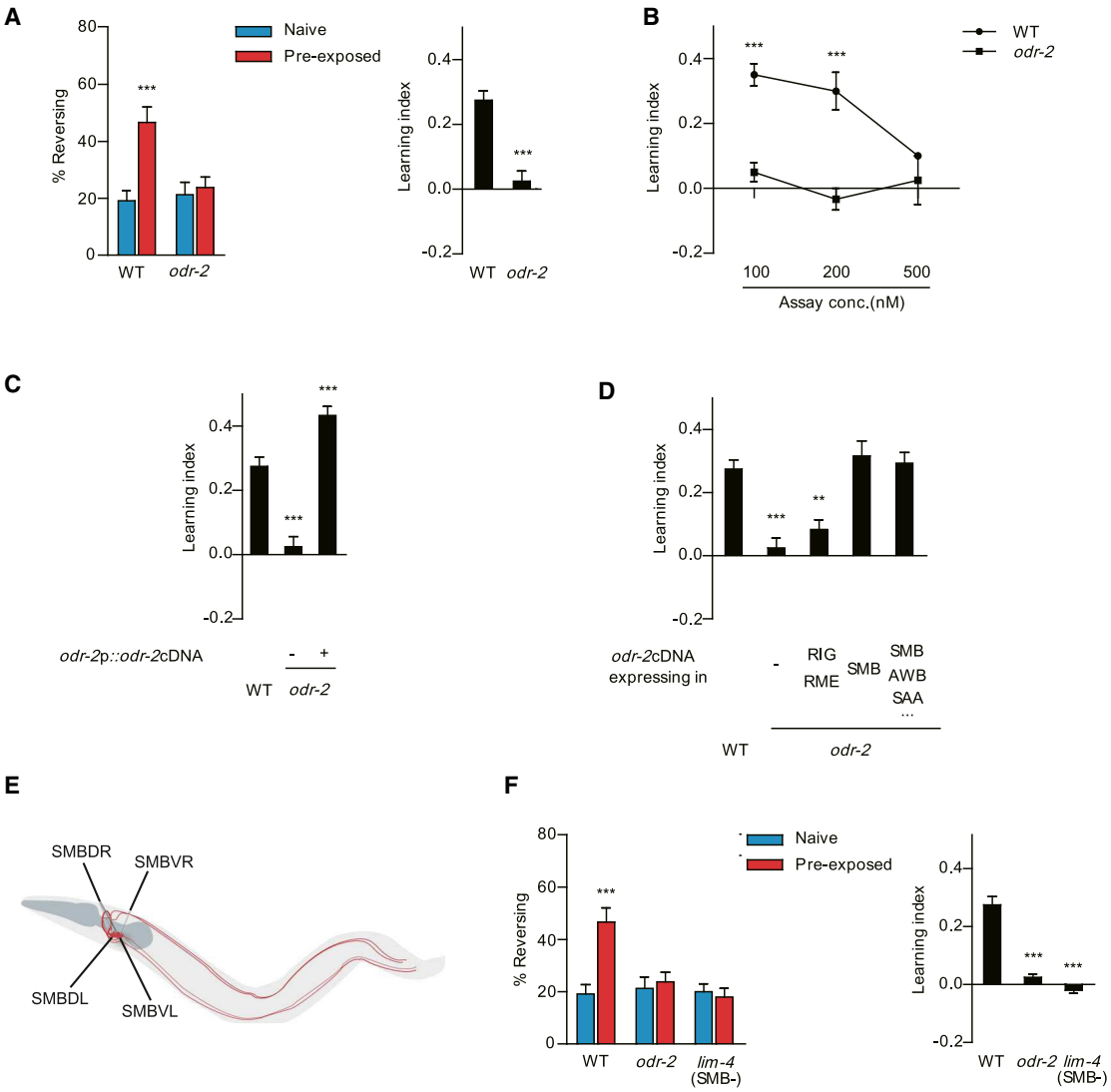

Figure 2. The Glycosylated Phosphatidylinositol-Linked Protein, ODR-2, Is Required for Increased ascr#3 Avoidance in ascr#3-Imprinted Animals

(A) Percentage of reversal (left) and learning index (right) in wild-type and *odr-2* mutants. *** indicates significantly different from naive (left) and wild-type (WT) (right) at $p < 0.001$ by one-way ANOVA with Bonferroni's post hoc test (left) and by Student's t test (right), respectively. n = 80–120 each.

(B) Learning index of wild-type and *odr-2* mutants at 100 nM, 200 nM, or 500 nM ascr#3. *** indicates different from wild-type at $p < 0.001$ by one-way ANOVA with Bonferroni's post hoc test. n = 30–60 each.

(C and D) Learning index of wild-type and *odr-2* mutants expressing *odr-2* cDNA under the control of *odr-2* promoter (RIG, RME, and SMB; C) or cell-specific promoters, including *odr-2* (−377) (RIG and RME), *flp-12* (−339) (SMB), and *lim-4* (AWB, SAA, RID, RIV, RMD, and SMB; D). ** and *** indicate different from wild-type at $p < 0.01$ and $p < 0.001$, respectively, by one-way ANOVA with Dunnett's post hoc test. (C) n = 80–120 each. (D) n = 60–140 each.

(E) Schematic diagram of the SMB neurons. A pair of dorsal and ventral cell bodies (SMBDs and SMBVs) are located in the head, and their processes innervate head muscle and run posteriorly.

(F) Percentage of reversal of naive and pre-exposed animals (left) and learning index (right) in wild-type, *odr-2*, and *lim-4* mutants. *** indicates different from naive (left) and wild-type (right) at $p < 0.001$ by one-way ANOVA with Bonferroni's (left) and Dunnett's post hoc tests (right), respectively. n = 80–120 each.

All error bars represent SEM. See also Figure S2.

rescue of the ascr#3 imprinting defects. We found that, whereas expression of *odr-2* in RIG and RME under the control of *odr-2* (−377) promoter [20] did not rescue these behavioral defects, ascr#3 imprinting defects were fully restored upon expression of *odr-2* exclusively in SMB under the control of *flp-12* (−339) promoter (Figure 2D) [20], indicating that ODR-2 acts in the SMB neurons to mediate ascr#3 imprinting.

The SMB neurons consist of two left and right pairs (dorsal or ventral) of sensory/inter/motor neuron types that are located in the head and that innervate the head and neck muscles (Figure 2E) [21]. Whereas their synapse-free processes extend along the ventral or dorsal sublateral cords to the tail, the SMB neurons have extensive electric and chemical synaptic contacts to other neurons in the head [21]. These neurons regulate head locomotion

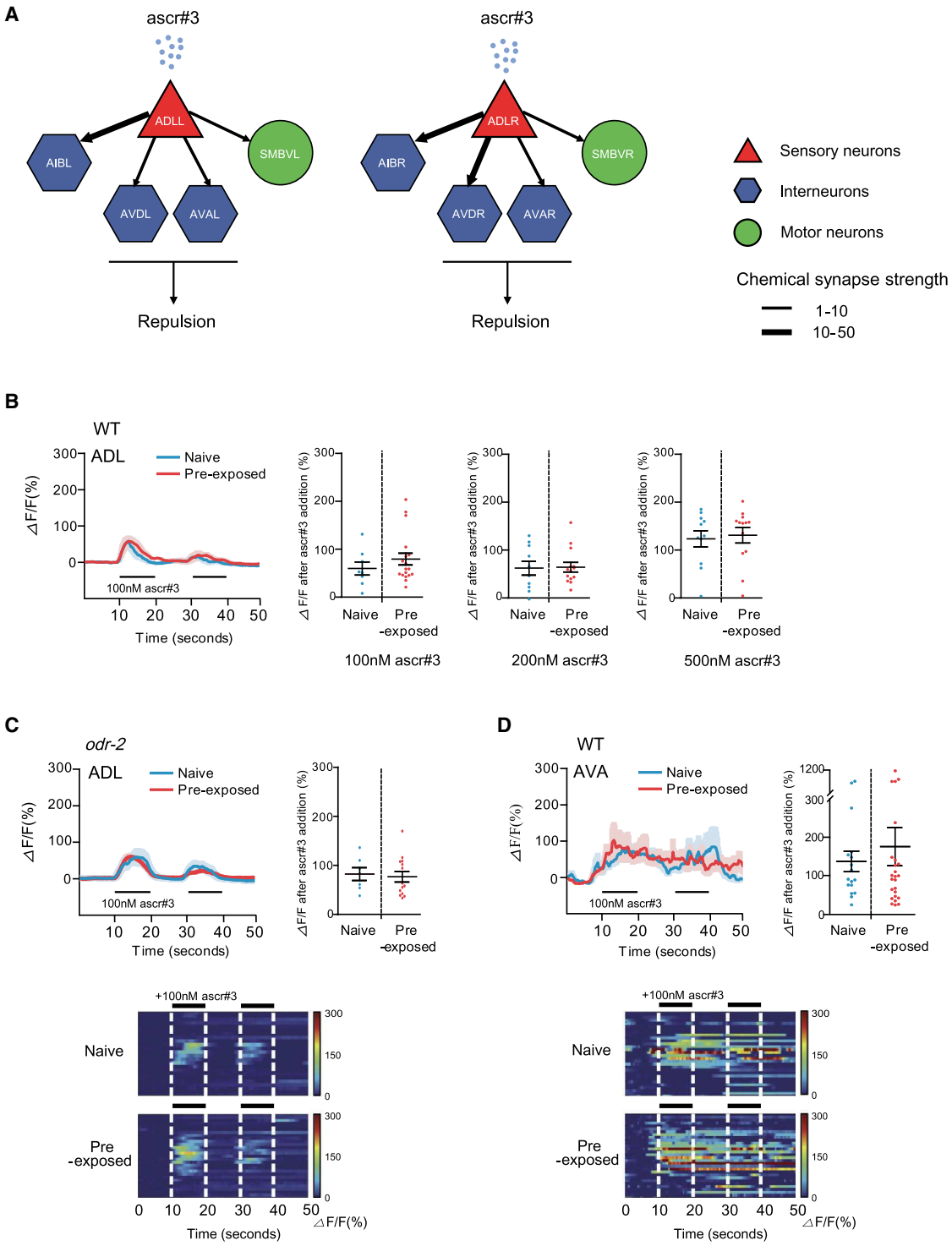

Figure 3. Ca^{2+} Response to Acute ascr#3 Exposure Is Not Altered in the ascr#3-Sensing ADL Neurons and Their Downstream Command Interneurons of ascr#3-Imprinted Animals

(A) Post-synaptic connections of the ADLL and ADLR neurons. The AIB, AVD, AVA, and SMBV neurons are post-synaptic to ADL. Chemical synapses between sensory (triangles), inter (hexagons), and motor (circles) are indicated as arrows. Synaptic strength is indicated in thickness of lines (http://www.wormwiring.org). (B) Ca^{2+} transients of ADL in response to 100 nM ascr#3 exposure. The average traces of Ca^{2+} responses during two pulses of 100 nM ascr#3 (left) and the maximum value of Ca^{2+} responses to 100 nM, 200 nM, or 500 nM ascr#3 (right) of naive (shown in blue) or pre-exposed animals (shown in red) in 50 s are shown. n = 8 (naive) and 18 (pre-exposed) each.

(legend continued on next page)

[20–22]. However, their roles in chemosensory behaviors have not been explored. We next investigated that the SMB neurons are required for ascr#3 imprinting. To address this issue, we examined *lim-4* mutants in which the SMB neurons are not fully differentiated and in which the functions of SMB are completely abolished [20]. *lim-4* mutants had been shown to exhibit additional defects, including neuronal specification [23]. Whereas *lim-4* mutants were still able to avoid ascr#3, pre-exposure to ascr#3 did not enhance ascr#3 avoidance in *lim-4* mutants (Figure 2F). These results together with *odr-2* rescue results support that the SMB neurons may play an important role in ascr#3 imprinting.

ascr#3-Induced Responses in the ADL Chemosensory Neurons Are Unaltered in ascr#3-Imprinted Worms

In adults, ascr#3 elicits avoidance behavior in hermaphrodites via the nociceptive ADL chemosensory neurons (Figure 3A) [7]. To describe the neuronal basis of pheromone imprinting, we first monitored intracellular Ca^{2+} dynamics in response to ascr#3 in transgenic animals expressing the genetically encoded calcium sensor GCaMP3 in the ascr#3-sensing ADL neurons. The ADL neurons exhibit a rapid and transient Ca^{2+} increase upon exposure to nano-molar concentrations of ascr#3 (Figure 3B) [7]. Both naive animals and ascr#3-imprinted animals displayed similar Ca^{2+} transients in adult ADL neurons upon addition of ascr#3 (Figure 3B). These results suggest that increased ascr#3 avoidance is not due to enhanced sensory responsiveness of ADL. Furthermore, consistent with the normal ascr#3 avoidance behavior of *odr-2* mutants, the ADL Ca^{2+} response to ascr#3 was not altered in *odr-2* mutants (Figure 3C).

The ADL sensory neurons drive ascr#3 avoidance through their chemical synapses [7]. Inspection of the anatomical wiring data from the *C. elegans* connectome suggests that ascr#3 signals from the ADL neurons are transmitted to a few major post-synaptic target neurons, including AIB (1st layer interneurons), and the AVA and AVD backward command interneurons (Figure 3A). Previous studies have shown that activity in AIB, AVA, and AVD is increased during backward movement or reversals [24]. We found that, whereas the AIB or AVD neurons exhibited noisy but low levels of Ca^{2+} responses upon exposure to ascr#3 (Figures S3A and S3B), the AVA cell bodies responded strongly and consistently to repeated ascr#3 addition with increased Ca^{2+} levels (Figure 3D). However, these responses were unaltered upon ascr#3 imprinting (Figures 3D, S3A, and S3B). These results imply that ascr#3 signals in the ADL neurons may be transmitted mainly via AVA but that imprinting does not enhance ascr#3 avoidance via this ADL-AVA circuit.

The SMB Neurons Mediate Increased ascr#3 Avoidance in ascr#3-Imprinted Animals

The *C. elegans* connectome data indicate that the SMBV neurons are additional post-synaptic partners of the ADL sensory neurons (Figure 3A), although the synaptic strength appears to be weak. Because the SMB neurons appear to play a role in ascr#3 imprinting, we then examined how SMB is involved in ascr#3-avoidance behavior.

We first expressed GCaMP3 in SMB under the control of *flp-12* (−339) promoter that drives transgene expression in all four SMB neurons [20]. We note that a SMBV-specific promoter is not currently available. Moreover, because the cell bodies of SMBD and SMBV are located in close proximity, differentiating among these neurons is challenging [20]. We thus examined ascr#3 responses in all SMB neurons together. Acute ascr#3 exposure did not elicit Ca^{2+} transients in the SMB neurons of naive control animals (Figure 4A; Movie S1). However, we detected consistent and robust Ca^{2+} transients in response to acute ascr#3 exposure in ascr#3-imprinted animals (Figure 4A; Movie S2). Because SMB may detect body muscle contractions that could be responsible for the observed Ca^{2+} responses in SMB, we paralyzed worms with the nicotinic acetylcholine receptor agonist levamisole. Levamisole-treated ascr#3-imprinted animals still exhibited similar or even enhanced Ca^{2+} dynamics upon ascr#3 exposure (Figure S4A).

To test whether the observed Ca^{2+} transients in SMB in ascr#3-imprinted animals are transmitted from ADL, we examined Ca^{2+} responses in transgenic animals expressing TeTx (tetanus toxin light chain) specifically in the ADL neurons to block synaptic transmission from ADL [7]. Ca^{2+} transients of SMB in ascr#3-imprinted animals were strongly suppressed by blocking ADL synaptic transmission (Figures 4B and S4B), suggesting that ascr#3 imprinting results in enhanced ascr#3 signal transmission from ADL to SMB. These results indicate that ascr#3 imprinting specifically alters the ADL-SMB synaptic transmission.

Moreover, the ascr#3-imprinting-dependent Ca^{2+} response in SMB was completely abolished in *odr-2* mutants (Figure 4C), indicating that *odr-2* elicits increased activity of SMB to ascr#3 exposure in imprinted animals by enhancing the ADL-SMB synaptic transmission.

Upregulation of *odr-2* Expression of L1 Larvae Is Sufficient for Increased ascr#3 Avoidance in Adults

To further investigate the role of *odr-2* in mediating increased SMB activity of ascr#3-imprinted animals, we monitored *odr-2* expression in SMB and found that *odr-2* expression in SMB was increased after transient exposure to ascr#3 at the L1 stage and was maintained through adulthood (Figure 4D). In contrast, *odr-2*p::*gfp* expression was unaffected in other *odr-2*-expressing cells, including RIG and RME (Figure 4D). To examine whether upregulation of *odr-2* at the L1 stage is sufficient for the increased ascr#3 avoidance in adults, we expressed *odr-2* cDNA in wild-type animals with the inducible expressed heat-shock promoter. Compared to animals with no heat-shock

(C) Ca^{2+} transients of ADL in response to 100 nM ascr#3 exposure in *odr-2* mutants. The average traces of Ca^{2+} responses during two pulses of 100 nM ascr#3 (left), heatmap of individual Ca^{2+} responses to ascr#3 (bottom), and the maximum value of Ca^{2+} responses to 100 nM ascr#3 (right) in naive (shown in blue) or pre-exposed (shown red) *odr-2* mutants are shown. n = 7 (naive) and 14 (pre-exposed) each.

(D) Ca^{2+} transients of AVA in response to 100 nM ascr#3 exposure. The average traces of Ca^{2+} responses during two pulses of 100 nM ascr#3 (left), heatmap of individual Ca^{2+} responses to ascr#3 (bottom), and the maximum value of Ca^{2+} responses to 100 nM ascr#3 (right) in naive (shown in blue) or pre-exposed animals (shown in red) are shown. n = 7 (naive) and 8 (pre-exposed) each.

All error bars represent SEM. See also Figure S3.

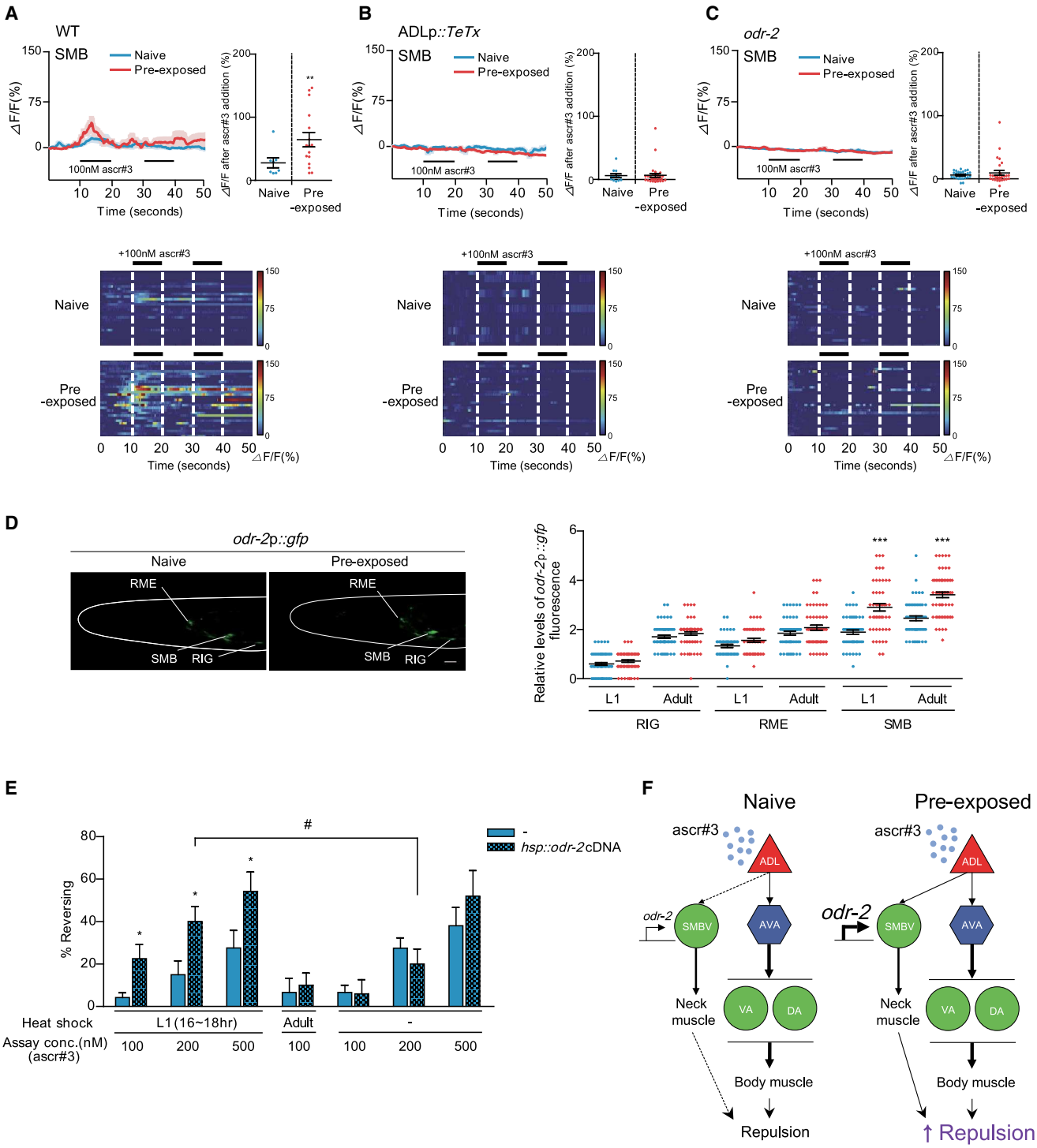

Figure 4. The SMB Motor Neurons Mediate Enhanced ascr#3 Avoidance in ascr#3-Imprinted Animals

(A–C) Ca^{2+} transients of the SMB neurons in response to 100 nM ascr#3 in wild-type animals (A), wild-type animals expressing ADLp::*TeTx* (B), or *odr-2* mutants (C). The average traces of Ca^{2+} responses during two pulses of 100 nM ascr#3 (left), heatmap of individual Ca^{2+} responses to ascr#3 (bottom), and the maximum value of Ca^{2+} responses to 100 nM ascr#3 (right) in naive (blue) or pre-exposed animals [10] are shown. ** indicates different from naive at $p < 0.01$ by Student's t test. n = 8–30 each.

(D) Representative images (left) and GFP quantification (right) of *odr-2*p::*gfp* expression in RIG, RME, and SMB of naive (shown in blue) and pre-exposed (shown in red) animals at the L1 or adult stages are shown. The images were taken of adults. *** indicates different from wild-type at $p < 0.001$ by one-way ANOVA with Bonferroni's post hoc test. n = 50–60 each. The scale bar represents 10 μm.

(legend continued on next page)

treated or those heat-shocked only at the adult stage, transient induction of *odr-2* gene activity at the L1 larval stage was sufficient to increase ascr#3 avoidance in adults (Figure 4E). Thus far, our results are consistent with a model in which the increased *odr-2* expression in SMB of the ascr#3-imprinted animals causes functional changes in the ADL-SMB synaptic activities.

DISCUSSION

The well-defined nervous system of *C. elegans* with only 302 neurons mediates a broad spectrum of behaviors. However, these behaviors are plastic and can be modulated by the animal's experience [25, 26]. For example, *C. elegans* is able to constantly monitor and adapt to their environment by forming short-term and/or long-term memories in their hard-wired neural circuits (see a review by [27]). *C. elegans* has also been shown to imprint long-term memories of environments, including odor or pathogen exposure experienced during development, via largely uncharacterized mechanisms [15, 17]. Here, we show a novel imprinting paradigm in *C. elegans*, where exposure of newly hatched animals to the ascr#3 pheromone increases adult neuronal activity in response to ascr#3, resulting in altered behavior. Because the long-lasting memory for ascr#3 pheromone is formed during a critical period of early development and shapes the ascr#3 avoidance behavior of adults, this learning and long-term memory process for the pheromone could be referred to as sensory imprinting [8]. Sensory imprinting is a form of long-term memory that occurs in many animals: for example, homing of salmon and neonatal attachment of rodents [28, 29]. This type of behavioral plasticity could be essential for animal survival in natural environments. ascr#3 is the most abundant and potent aversive pheromone in *C. elegans* hermaphrodites and may represent conditions of overcrowding [7, 30, 31]. Thus, newly hatched worms may pair this specific ascr#3 pheromone memory to their neuronal activity to promote searching behavior for more favorable environments as adults or to shape currently unidentified behavioral or physiological states for optimal fitness.

We previously showed that the ADL sensory neurons detect *C. elegans* pheromone ascr#3 and drive ascr#3 avoidance through their chemical synapses [7]. The ADL neurons directly connect to more than twenty post-synaptic neurons, and inspection of the anatomical wiring data, including the number of synapses, led us to hypothesize that ascr#3 signals from ADL are transmitted to the three major post-synaptic target neurons, including the AIB, AVA, and AVD interneurons. In this work, we have found that, under non-ascr#3 pre-exposed (naive) conditions, the ascr#3 signals are transmitted via the ADL-AVA synapses (Figure 4F). However, whereas transient exposure to ascr#3 at the L1 larval stage does not appear to affect this ADL-AVA synaptic transmission, this experience instead increases the ADL-SMB synaptic activities that are normally inactive in naive animals and may account for the observed enhanced ascr#3-avoidance behavior in adult worms (Figure 4F).

The conclusion that the SMB neurons are the critical site for mediating ascr#3 imprinting is supported by these findings: (1) the SMB neurons respond to ascr#3 exposure in ascr#3-imprinted, but not in naive, animals; (2) expression of *odr-2* that is necessary and partly sufficient for ascr#3 imprinting is increased specifically in SMB of ascr#3-imprinted animals; and (3) *lim-4* mutants in which SMB functions are abolished fail to imprint ascr#3 experience. Laser ablation of the SMB motor neurons causes increased reversal frequency and wave amplitude of forward locomotion [20, 22]. Because the SMB neurons innervate head and neck muscles and ascr#3 exposure now activates the SMB neurons in ascr#3-imprinted animals, our results suggest that early ascr#3 experience causes the SMB neurons to sensitize to subsequent ascr#3 exposure and modulate backward movement via the alteration of head/neck muscle activity (Figure 4F). For example, in addition to body muscle contraction triggered by ADL-AVA synaptic transmission, head/neck muscle contraction due to enhanced SMB neuronal activities upon ascr#3 imprinting may increase reversal rates further [24, 32] or the SMB neurons could directly activate backward motor circuits via interneurons, including the SAA neurons [21].

Our data show that *odr-2* is essential for ascr#3 imprinting. *odr-2* encodes a novel protein distantly related to murine Ly6 lymphocyte antigen protein that is tethered to membrane by a GPI anchor [19]. In vertebrates, GPI-anchored proteins have roles in development and neurogenesis by regulating several signaling pathways, including Notch, Wnt, or transforming growth factor β (TGF-β) [33]. Moreover, a set of Ly6-related genes, including Lynx1 and Lynx2, have been shown to be expressed in the nervous system and appear to be accessory components of nicotinic acetylcholine receptors, thus modulating their functions [34, 35]. Our results indicate that the ODR-2 GPI-anchored protein changes synaptic activity between ADL and SMB. ODR-2 proteins are localized on cell bodies and neuronal processes [36]. Thus, it is possible that ODR-2 may be co-localized with and regulate functions of neurotransmitter receptors in SMB.

Understanding how individual synapses are functionally or anatomically altered upon sensory imprinting is the essential first steps toward being able to dissect molecular and neuronal mechanisms underlying sensory imprinting and other forms of behavioral plasticity. Given that structures and functions of neural circuits are evolutionarily conserved, we expect that our work will lead to a general framework for understanding how circuits are modulated in higher animals, including humans.

(E) Percentage of reversal of adult transgenic animals expressing *hsp*::*odr-2* cDNA under heat shock at the L1 and adult stages. * indicates different from *hsp*::*odr-2* cDNA (−), and # indicates different from no heat shock at $p < 0.05$ by Student's t test. n = 50–70 each.

(F) Model for circuit mechanisms underlying ascr#3 avoidance in naive or ascr#3-imprinted animals. In naive animals, ADL detects ascr#3 and transmits the signals to the post-synaptic AVA command interneurons and downstream VA/DA motor neurons. In pre-exposed animals, the increased expression of *odr-2* in SMB initiates synaptic transmission from ADL to SMB that mediate ascr#3 signal transmission from ADL not only to AVA but SMB. SMB activation may serve to sensitize background for backward movement via excitation of head muscles.

In (A)–(E), error bars represent SEM. See also Figure S4.

STAR★METHODS

Detailed methods are provided in the online version of this paper and include the following:

- KEY RESOURCES TABLE
- CONTACT FOR REAGENT AND RESOURCE SHARING
- EXPERIMENTAL MODEL AND SUBJECT DETAILS
- METHOD DETAILS
  - Generation of *C. elegans* transgenic lines
  - Pheromone imprinting
  - Post-dauer assay
  - Behavioral assay
  - In vivo calcium imaging
  - Levamizole treatment
  - Heat shock treatment
- QUANTIFICATION AND STATISTICAL ANALYSIS
  - Representative images
  - GFP quantification
  - Statistical tests

SUPPLEMENTAL INFORMATION

Supplemental Information includes four figures and two movies and can be found with this article online at http://dx.doi.org/10.1016/j.cub.2017.08.068.

AUTHOR CONTRIBUTIONS

M.H., L.R., M.C.O., and A.R.J. performed the experiments; J.K., S.C., R.A.B., and H.C. provided reagents; M.H., L.R., M.C.O., Y.H.H., K.J.L., P.S., S.E.H., and K.K. analyzed and interpreted data; and M.H., L.R., P.S., S.E.H., and K.K. wrote the manuscript.

ACKNOWLEDGMENTS

We are grateful to Yishi Jin for reagents, the Caenorhabditis Genetics Center (NIH Office of Research Infrastructure Programs; P40 OD010440), and the National BioResource Project (Japan) for strains and Seung-Jae V. Lee, Sunkyung Lee, and members of the S.V. Lee and K. Kim lab for helpful discussion and/or critical comments on the manuscript. We also thank members of the Advanced Neural Imaging Center in KBRI for their technical support. This work was supported by the DGIST R&D Program of the Ministry of Science, ICT and Future Planning (17-BD-06), KBRI Basic Research Program of the Ministry of Science, ICT and Future Planning (17-BR-04), and National Research Foundation of Korea (NRF-2015R1D1A1A09061430 and NRF-2017R1A4A1015534) (K.K.); NIH R15GM111094 (S.E.H.); NIH R01GM087533 (R.A.B.); NSF IOS 1256488 and NSF IOS 1655118 (P.S.); KBSI grant T37416 (Y.H.H.); and the KBRI Basic Research Program of the Ministry of Science, ICT and Future Planning (17-BR-02) and Korea Health Technology R&D Project of the Ministry for Health and Welfare grant HI14C1135 (K.J.L.).

Received: June 15, 2017
Revised: August 7, 2017
Accepted: August 29, 2017
Published: October 5, 2017

REFERENCES

1. Beach, F.A., and Jaynes, J. (1954). Effects of early experience upon the behavior of animals. Psychol. Bull. *51*, 239–263.
2. Hensch, T.K. (2004). Critical period regulation. Annu. Rev. Neurosci. *27*, 549–579.
3. Jeong, P.Y., Jung, M., Yim, Y.H., Kim, H., Park, M., Hong, E., Lee, W., Kim, Y.H., Kim, K., and Paik, Y.K. (2005). Chemical structure and biological activity of the Caenorhabditis elegans dauer-inducing pheromone. Nature *433*, 541–545.
4. Butcher, R.A., Fujita, M., Schroeder, F.C., and Clardy, J. (2007). Small-molecule pheromones that control dauer development in Caenorhabditis elegans. Nat. Chem. Biol. *3*, 420–422.
5. Macosko, E.Z., Pokala, N., Feinberg, E.H., Chalasani, S.H., Butcher, R.A., Clardy, J., and Bargmann, C.I. (2009). A hub-and-spoke circuit drives pheromone attraction and social behaviour in C. elegans. Nature *458*, 1171–1175.
6. Edison, A.S. (2009). Caenorhabditis elegans pheromones regulate multiple complex behaviors. Curr. Opin. Neurobiol. *19*, 378–388.
7. Jang, H., Kim, K., Neal, S.J., Macosko, E., Kim, D., Butcher, R.A., Zeiger, D.M., Bargmann, C.I., and Sengupta, P. (2012). Neuromodulatory state and sex specify alternative behaviors through antagonistic synaptic pathways in C. elegans. Neuron *75*, 585–592.
8. Lorenz, K. (1935). Der Kumpan in der Umwelt des Vogels. J. Ornithol. *83*, 137–213.
9. Hilliard, M.A., Bargmann, C.I., and Bazzicalupo, P. (2002). C. elegans responds to chemical repellents by integrating sensory inputs from the head and the tail. Curr. Biol. *12*, 730–734.
10. Srinivasan, J., Kaplan, F., Ajredini, R., Zachariah, C., Alborn, H.T., Teal, P.E., Malik, R.U., Edison, A.S., Sternberg, P.W., and Schroeder, F.C. (2008). A blend of small molecules regulates both mating and development in Caenorhabditis elegans. Nature *454*, 1115–1118.
11. Sims, J.R., Ow, M.C., Nishiguchi, M.A., Kim, K., Sengupta, P., and Hall, S.E. (2016). Developmental programming modulates olfactory behavior in C. elegans via endogenous RNAi pathways. eLife *5*, e11642.
12. Hall, S.E., Beverly, M., Russ, C., Nusbaum, C., and Sengupta, P. (2010). A cellular memory of developmental history generates phenotypic diversity in C. elegans. Curr. Biol. *20*, 149–155.
13. Hall, S.E., Chirn, G.W., Lau, N.C., and Sengupta, P. (2013). RNAi pathways contribute to developmental history-dependent phenotypic plasticity in C. elegans. RNA *19*, 306–319.
14. L'Etoile, N.D., Coburn, C.M., Eastham, J., Kistler, A., Gallegos, G., and Bargmann, C.I. (2002). The cyclic GMP-dependent protein kinase EGL-4 regulates olfactory adaptation in C. elegans. Neuron *36*, 1079–1089.
15. Remy, J.J., and Hobert, O. (2005). An interneuronal chemoreceptor required for olfactory imprinting in C. elegans. Science *309*, 787–790.
16. Ikeda, D.D., Duan, Y., Matsuki, M., Kunitomo, H., Hutter, H., Hedgecock, E.M., and Iino, Y. (2008). CASY-1, an ortholog of calsyntenins/alcadeins, is essential for learning in Caenorhabditis elegans. Proc. Natl. Acad. Sci. USA *105*, 5260–5265.
17. Jin, X., Pokala, N., and Bargmann, C.I. (2016). Distinct circuits for the formation and retrieval of an imprinted olfactory memory. Cell *164*, 632–643.
18. Bargmann, C.I., Hartwieg, E., and Horvitz, H.R. (1993). Odorant-selective genes and neurons mediate olfaction in C. elegans. Cell *74*, 515–527.
19. Chou, J.H., Bargmann, C.I., and Sengupta, P. (2001). The Caenorhabditis elegans odr-2 gene encodes a novel Ly-6-related protein required for olfaction. Genetics *157*, 211–224.
20. Kim, J., Yeon, J., Choi, S.K., Huh, Y.H., Fang, Z., Park, S.J., Kim, M.O., Ryoo, Z.Y., Kang, K., Kweon, H.S., et al. (2015). The evolutionarily conserved LIM homeodomain protein LIM-4/LHX6 specifies the terminal identity of a cholinergic and peptidergic C. elegans sensory/inter/motor neuron-type. PLoS Genet. *11*, e1005480.
21. White, J.G., Southgate, E., Thomson, J.N., and Brenner, S. (1986). The structure of the nervous system of the nematode Caenorhabditis elegans. Philos. Trans. R. Soc. Lond. B Biol. Sci. *314*, 1–340.
22. Gray, J.M., Hill, J.J., and Bargmann, C.I. (2005). A circuit for navigation in Caenorhabditis elegans. Proc. Natl. Acad. Sci. USA *102*, 3184–3191.
23. Sagasti, A., Hobert, O., Troemel, E.R., Ruvkun, G., and Bargmann, C.I. (1999). Alternative olfactory neuron fates are specified by the LIM homeobox gene lim-4. Genes Dev. *13*, 1794–1806.

24. Piggott, B.J., Liu, J., Feng, Z., Wescott, S.A., and Xu, X.Z. (2011). The neural circuits and synaptic mechanisms underlying motor initiation in C. elegans. Cell *147*, 922–933.
25. de Bono, M., and Maricq, A.V. (2005). Neuronal substrates of complex behaviors in C. elegans. Annu. Rev. Neurosci. *28*, 451–501.
26. Giles, A.C., Rose, J.K., and Rankin, C.H. (2006). Investigations of learning and memory in Caenorhabditis elegans. Int. Rev. Neurobiol. *69*, 37–71.
27. Ardiel, E.L., and Rankin, C.H. (2010). An elegant mind: learning and memory in Caenorhabditis elegans. Learn. Mem. *17*, 191–201.
28. Nevitt, G.A., Dittman, A.H., Quinn, T.P., and Moody, W.J., Jr. (1994). Evidence for a peripheral olfactory memory in imprinted salmon. Proc. Natl. Acad. Sci. USA *91*, 4288–4292.
29. Wilson, D.A., and Sullivan, R.M. (1994). Neurobiology of associative learning in the neonate: early olfactory learning. Behav. Neural Biol. *61*, 1–18.
30. Golden, J.W., and Riddle, D.L. (1982). A pheromone influences larval development in the nematode Caenorhabditis elegans. Science *218*, 578–580.
31. Izrayelit, Y., Robinette, S.L., Bose, N., von Reuss, S.H., and Schroeder, F.C. (2013). 2D NMR-based metabolomics uncovers interactions between conserved biochemical pathways in the model organism Caenorhabditis elegans. ACS Chem. Biol. *8*, 314–319.
32. Guo, Z.V., Hart, A.C., and Ramanathan, S. (2009). Optical interrogation of neural circuits in Caenorhabditis elegans. Nat. Methods *6*, 891–896.
33. Fujihara, Y., and Ikawa, M. (2016). GPI-AP release in cellular, developmental, and reproductive biology. J. Lipid Res. *57*, 538–545.
34. Miwa, J.M., Ibanez-Tallon, I., Crabtree, G.W., Sánchez, R., Sali, A., Role, L.W., and Heintz, N. (1999). lynx1, an endogenous toxin-like modulator of nicotinic acetylcholine receptors in the mammalian CNS. Neuron *23*, 105–114.
35. Tekinay, A.B., Nong, Y., Miwa, J.M., Lieberam, I., Ibanez-Tallon, I., Greengard, P., and Heintz, N. (2009). A role for LYNX2 in anxiety-related behavior. Proc. Natl. Acad. Sci. USA *106*, 4477–4482.
36. Gottschalk, A., and Schafer, W.R. (2006). Visualization of integral and peripheral cell surface proteins in live Caenorhabditis elegans. J. Neurosci. Methods *154*, 68–79.
37. Brenner, S. (1974). The genetics of Caenorhabditis elegans. Genetics *77*, 71–94.
38. Coates, J.C., and de Bono, M. (2002). Antagonistic pathways in neurons exposed to body fluid regulate social feeding in Caenorhabditis elegans. Nature *419*, 925–929.
39. Tian, L., Hires, S.A., Mao, T., Huber, D., Chiappe, M.E., Chalasani, S.H., Petreanu, L., Akerboom, J., McKinney, S.A., Schreiter, E.R., et al. (2009). Imaging neural activity in worms, flies and mice with improved GCaMP calcium indicators. Nat. Methods *6*, 875–881.
40. Kim, K., Sato, K., Shibuya, M., Zeiger, D.M., Butcher, R.A., Ragains, J.R., Clardy, J., Touhara, K., and Sengupta, P. (2009). Two chemoreceptors mediate developmental effects of dauer pheromone in C. elegans. Science *326*, 994–998.
41. Srinivasan, J., Durak, O., and Sternberg, P.W. (2008). Evolution of a polymodal sensory response network. BMC Biol. *6*, 52.
42. Ibsen, S., Tong, A., Schutt, C., Esener, S., and Chalasani, S.H. (2015). Sonogenetics is a non-invasive approach to activating neurons in Caenorhabditis elegans. Nat. Commun. *6*, 8264.
43. Chronis, N., Zimmer, M., and Bargmann, C.I. (2007). Microfluidics for in vivo imaging of neuronal and behavioral activity in Caenorhabditis elegans. Nat. Methods *4*, 727–731.
44. Kratsios, P., Stolfi, A., Levine, M., and Hobert, O. (2011). Coordinated regulation of cholinergic motor neuron traits through a conserved terminal selector gene. Nat. Neurosci. *15*, 205–214.

STAR★METHODS

KEY RESOURCES TABLE

REAGENT or RESOURCE	SOURCE	IDENTIFIER
Chemicals, Peptides, and Recombinant Proteins		
Levamisole	Sigma	Cat# 16595-80-5
ascr#3	This paper	
Critical Commercial Assays		
PDMS Sylgard 184 Silicone Elastomer Kit	Dow Corning	Product code: 1064291
Experimental Models: Organisms/Strains		
odr-2(n2145) V	*Caenorhabditis* Genetics Center	RRID: WB-STRAIN:CX2304
odr-2(n2145) V ; *lskEx606[odr-2Δ3p::odr-2*cDNA*]*	This paper	N/A
odr-2(n2145) V; *lskEx607[flp-12Δ3p::odr-2*cDNA*]*	This paper	N/A
odr-2(n2145) V; *lskEx608[lim-4p::odr-2*cDNA*]*	This paper	N/A
lim-4(ky403) X	*Caenorhabditis* Genetics Center	RRID: WB-STRAIN:CX3937
lskEx218[sre-1p::GCaMP3; unc-122p:dsRed]	This paper	N/A
odr-2(n2145) V; *lskEx218[sre-1p::GCaMP3; unc-122p:dsRed]*	This paper	N/A
lskEx597[nmr-1p::GCaMP3; unc-122p::dsRed]	This paper	N/A
lsk Ex113[flp-12Δ3p::GCaMP3; unc-122p::dsRed]	This paper	N/A
lskEx611[sre-1p::TeTx; unc-122p::gfp]; lskEx113[flp12Δ3p::GCaMP3]	This paper	N/A
odr-2(n2145) V; *lskEx113[flp-12Δ3p::GCaMP3]*	This paper	N/A
lsk ls11[odr-2p::gfp; unc-122p::dsRed]	This paper	N/A
*lskEx418[hsp::odr-2*cDNA*; unc-122p::gfp]*	This paper	N/A
lskEx895 [avr-14p::gfp; unc-122p::dsRed]; lskEx28 [flp-12p::mcherry; unc-122p::gfp]	This paper	N/A
odr-2(n2145); lskEx895 [avr-14p::gfp; unc-122p::dsRed]; lskEx28 [flp-12p::mcherry; unc-122p::gfp]	This paper	N/A
egl-4(ks60) IV	*Caenorhabditis* Genetics Center	RRID: WB-STRAIN:FK223
sra-11(ok630) II	*Caenorhabditis Genetics* Center	RRID: WB-STRAIN:RB816
odr-3(n2150) V	*Caenorhabditis* Genetics Center	RRID: WB-STRAIN:CX2205
odr-7(ky4) X	*Caenorhabditis* Genetics Center	RRID: WB-STRAIN:CX4
odr-10(ky32) X	*Caenorhabditis* Genetics Center	RRID: WB-STRAIN:CX32
casy-1(tm718) II	National BioResource Project	N/A
casy-1(pe401) II	*Caenorhabditis* Genetics Center	RRID: WB-STRAIN:JN414
ttx-3(ks5) X	*Caenorhabditis* Genetics Center	RRID: WB-STRAIN:FK134
tdc-1(n3419) II	*Caenorhabditis* Genetics Center	RRID: WB-STRAIN:MT13113
lskEx610[npr-9p::GCaMP3; unc-122p::dsRed]	This paper	N/A
Software and Algorithms		
AxioVision software	Zeiss	RRID: SCR_002677
ZEN 2010 Lite Edition software	Zeiss	RRID: SCR_013672
ImageJ	https://imagej.nih.gov/ij/	RRID: SCR_003070
MATLAB	MathWorks	RRID: SCR_001622
Prism 5.0	GraphPad Software	RRID: SCR_002798
Adobe Illustrator CS6	Adobe	RRID: SCR_014198

CONTACT FOR REAGENT AND RESOURCE SHARING

Further information and requests for resources and reagents should be directed to and will be fulfilled by the Lead Contact, Dr. Kyuhyung Kim (khkim@dgist.ac.kr).

EXPERIMENTAL MODEL AND SUBJECT DETAILS

C. elegans N2 strain was used as wild-type. Wild-type and transgenic animals were maintained at 20°C with abundant *E. coli* OP50 as food following standard conditions [37]. Day 1 (~24 hr after mid-L4 larval stage) young adult, hermaphrodite animals were used for experimentation, with the exception of the *odr-2*p*::gfp* quantification study in which the L1 stage animals were also assayed (Figure 4D).

METHOD DETAILS

Generation of *C. elegans* transgenic lines

odr-2 18a cDNA was amplified with a set of primers containing restriction sites, 5′-*Age*I and 3′-*Not*I using PCR and inserted into pMC10 for performing the *odr-2* rescue experiment [19]. Upstream regulatory sequences, including *odr-2* (RIG, RME and SMB), *odr-2* (−377) (RIG and RME), *flp-12* (−339) (SMB), and *lim-4* (AWB, SAA, RID, RIV, RMD and SMB), were fused with *odr-2*cDNA to drive its expression in specific neurons [20]. To generate the *hsp::odr-2*cDNA transgene, the *hsp16.2* promoter was amplified from the *hsp16.2*p*::unc-3*cDNA transgene [38].

For Ca^{2+} imaging experiments of the AIB, AVD and AVA neurons, the promoter region of *sre-1*p*::GCaMP3* transgene was exchanged with *npr-9* (AIB) or *nmr-1* (AVD and AVA) promoters [7, 39]. *nmr-1p* was amplified from pCZGY1553 (a kind gift from Yishi Jin), and *npr-9*p was 2076 bp of upstream regulatory sequence amplified from genomic DNA by PCR. These promoters were ligated with GCaMP3 using the restriction sites, *Hind*III and BamHI.

Each transgenic *C. elegans* strain was generated by microinjection of the rescue construct (10 ng/μl) with *unc-122*p*::dsRed* (50 ng/μl). The *hsp::odr-2*cDNA construct was injected with the *unc-122*p*::gfp* marker (50 ng/μl).

Pheromone imprinting

For pheromone imprinting, two types of 35 mm noble agar plates seeded with *E. coli* OP50 were made: the negative control plate contained distilled water (naive) and the experimental plate contained pheromones (pre-exposed). Figures 1G and 1H utilized experimental plates containing 600 nM ascr#3, ascr#2 and ascr#5, and 600 nM ascr#3, ascr#2, ascr#5 and icas#9, respectively. All other assays in this study used experimental plates containing 600 nM ascr#3 for imprinting. To pre-expose animals to ascr#3, five 1-day-old young adult hermaphrodites were placed onto each control and experimental plate for 2~3 hr until 30 to 50 eggs were laid. After 1 day (~26 hr), the naive or pre-exposed L1 stage animals were transferred onto 60 mm nematode growth media plates seeded with *E. coli* OP50 food and grown for 2.5 days until the young adult stage. For male imprinting experiments, we added ~20 males with L4 hermaphrodites for 1 day to mate and picked 5 adult hermaphrodites onto each naive and pre-exposed plates. For imprinting analysis of the next generation, 5 adults from naive or pre-exposed group (P0) were placed onto new control plates and allowed to lay 30~50 eggs (F1). The adults were then subsequently removed and the plates were incubated for 2.5 days at 20°C.

Post-dauer assay

Dauer formation assay was based on the protocol in [40]. 20 μL heat-killed OP50 was seeded onto 3.5 mm 600 nM ascr#3 noble agar plates. 5~10 young adults were placed and discarded when over 50 eggs were obtained. The eggs were grown at 25°C for 68~72hr. Animals in dauer formation were picked onto new OP50 seeded 60 mm plates and grown at 20°C for 2~3 days. We assayed ascr#3 avoidance with adult animals which were grown at 20°C as control.

Behavioral assay

The drop assay was performed as described with modifications [7]. All behavioral assays were performed in the absence of food and used 100 nM ascr#3 diluted in M13 buffer (30 mM Tris-HCl [pH 7.0], 100 mM NaCl, 10 mM KCl), except Figure S1D which 200 mM glycerol was used [41]. To measure the percent of animals reversing upon ascr#3 exposure, a young adult was transferred onto a plate without food and M13 buffer was dropped near the head of worm. If the worm failed to reverse in response to M13 after 10 s, ascr#3 was dropped onto the front of the head and avoidance behaviors (reversal) were monitored for 10 s. Short or long reversals were defined as reversals with fewer than two head bends or more than two head bends, respectively [42]. Long reversals were counted as repulsion in this study. The imprinting index was calculated as the percentage of reversals of pre-exposed animals minus percentage of reversals of naive animals. Each assay tested the avoidance response of 10 young adult hermaphrodite animals, and at least 3 independent trials were performed.

In vivo calcium imaging

Calcium imaging experiments were performed as described previously [7], using microfluidics chips that were produced in-house with a custom made chrome mask and master mold [43]. Briefly, PDMS Sylgard 184 Silicone Elastomer Kit (Dow Corning) was solidified on the master mold at 70°C for 2 hr, and then was attached on a 24 × 24 mm glass coverslip using CUTE plasma equipment (Air) (FEMTOSCIENCE). The *C. elegans* transgenic strains used for calcium imaging experiments included *sre-1*p*::GCaMP3* (ADL), *flp-12* (−339)p*::GCaMP3* (SMB), *npr-9*p*::GCaMP3* (AIB) and *nmr-1*p*::GCaMP3* (AVA and AVD) were used [7]. Each animal was

exposed to fluorescent light for 1∼2 min and the images were captured under fixed exposure time (100ms) for 1 min with Zeiss Axioplan microscope using a 40X objective and a Zeiss AxioCam HR. The images were analyzed by AxioVision software, ImageJ, and custom-written scripts in MATLAB [7].

Levamizole treatment

25 mM levamisole (Sigma) was used to paralyze animals. 25 mM levamisole was diluted in M9 buffer from 0.25 M levamisole. The animals were placed into the solution for about 1 min, during which pharyngeal pumping ceased, indicating paralysis.

Heat shock treatment

Heat shock treatment was performed as previously described [44]. After 16 hr from egg laying, animals were twice exposed to a 33°C heat shock for 30 min with a 1 hr recovery at 20°C in between. After the second heat shock treatment, the worms were incubated at 20°C until the adult stage and behavioral assays were performed (see above).

QUANTIFICATION AND STATISTICAL ANALYSIS

Representative images

Images in Figures 4D and 4G were acquired using a Zeiss LSM700 Confocal microscope and Zeiss LSM780 Confocal microscope, respectively. The images were taken and analyzed through ZEN 2010 and ImageJ.

GFP quantification

For GFP quantification, the animals were anaesthetized by using 1 M NaN_3 and placed on 2% agarose pad with a 24 × 24 mm coverslip. *odr-2p::gfp* strain was integrated using UV crosslinker (UVP). A minimum of 30 *odr-2p::gfp* animals were exposed to 100 mM ascr#3 or control plates at the L1 larval stage following the imprinting protocol described above and quantified for GFP fluorescence. GFP expression was scored under 40X objective Zeiss Axioplan microscopy by observing the brightness of the neuron cell body and process. The animals were observed under 40X objective Zeiss Axioplan microscopy and LSM700 Confocal microscope. The images were taken and acquired by AxioVision or Zen 2010. All strains were assayed in parallel in two independent experiments.

Statistical tests

All of statistics was analyzed using Prism 5.0. When only two groups were compared, two tailed unpaired Student's t test was used. One-way ANOVA test was utilized to evaluate variation among more than two groups of datasets. The post hoc tests used include Dunnett's test for multiple comparisons obtained at the same experimental condition, and Bonferroni's test when the multiple comparisons were made from data produced at different conditions. All error bars indicate SEM. Detailed information of each statistical analysis is described in the figure legends.